

Diffusive photospheres in gamma-ray bursts

G. V. Vereshchagin^{1,2,3,4} and I. A. Siutsou^{3,5}

¹*ICRANet, 65122, p.le della Repubblica, 10, Pescara, Italy*

²*ICRA and Dipartimento di Fisica, Sapienza Università di Roma, P.le Aldo Moro 5, 00185 Rome, Italy*

³*ICRANet-Minsk, National Academy of Sciences of Belarus, Nezavisimosti ave. 68, 220072 Minsk, Belarus*

⁴*INAF, Viale del Parco Mellini 84, 00136 Rome, Italy*

⁵*Institute of Physics of Belarus NAS, Nezavisimosti Avenue 68, Minsk 220072, Belarus*

26 March 2020

Key words: radiation mechanisms: thermal γ radiative transfer γ gamma-ray burst: transients

ABSTRACT

Photospheric emission may originate from relativistic outflows in two qualitatively different regimes: last scattering of photons inside the outflow at the photospheric radius, or radiative diffusion to the boundary of the outflow. In this work the measurement of temperature and flux of the thermal component in the early afterglows of several gamma-ray bursts (GRBs) along with the total flux in the prompt phase are used to determine initial radii of the outflow as well as its Lorentz factors. Results indicate that in some cases the outflow has relatively low Lorentz factors $\Gamma < 10$, favouring cocoon interpretation, while in other cases Lorentz factors are larger $\Gamma > 10$, indicating diffusive photospheric origin of the thermal component, associated with an ultrarelativistic outflow.

1 INTRODUCTION

Gamma-ray bursts (GRBs) are strong and short flashes of hard radiation originating at cosmological distances. Since their discovery a number of dedicated space observatories and ground based telescopes are constantly monitoring the sky daily reporting new bursts and measuring distance to their host galaxies. GRBs come in two kinds: short and long, with their possible progenitors being binary neutron star mergers and collapsing massive stars reaching the endpoint of their evolution, respectively. Observed emission in GRBs is well separated in two distinct episodes: brief and highly irregular prompt phase with dominant hard X-ray and γ -radiation, and smoothly decaying long lasting afterglow emission with broadband spectra, ranging from radio waves up to sub-TeV energies. Extremely large energies released in γ -rays ($\leq 10^{54}$ erg) as well as a short variability time (≤ 10 ms) point to ultrarelativistic outflows giving rise to the observed emission (Zhang 2018).

Prompt emission spectra are non-thermal, their origin is usually associated with the synchrotron mechanism in relativistic shock waves (Rees & Meszaros 1994). Photospheric models with possible dissipation of kinetic energy of the outflow are attractive alternative to the synchrotron models since observation of thermal radiation allows determination of basic hydrodynamic characteristics of the outflow from which these bursts originate (Vereshchagin 2014; Pe'er & Ryde 2017). The photons in these models are trapped and advected with the outflow until it becomes transparent. In many GRBs subdominant thermal component was detected during their prompt emission, while in several GRB 090902B observed spectrum is almost thermal (Ryde et al. 2010, 2017).

Thermal components are also detected in time resolved spectra

during the early afterglow in a number of GRBs (Page et al. 2011; Starling et al. 2012; Sparre & Starling 2012; Friis & Watson 2013; Valan et al. 2018; Izzo et al. 2019). So far several mechanisms to generate such emission are proposed. They include a shock breakout from a progenitor star or a stellar wind (Campana et al. 2006) and a hot cocoon formed when the relativistic jet emerges from the stellar surface (Pe'er et al. 2006; Nakar & Piran 2017). Some authors argue that shock breakouts are not energetic enough and do not last long enough to explain observed thermal emission (Valan et al. 2018), leaving cocoons as a favourite model. In addition, there is an alternative proposal of a cloud or a clump with small mass, accelerated by the GRB outflow (Ruffini et al. 2017).

Most papers dealing with the photospheric emission, e.g. (Mészáros & Rees 2000; Pe'er 2008; Pe'er & Ryde 2011; Beloborodov 2011; Lundman et al. 2013; Santana et al. 2016; Bhat-tacharya et al. 2018), for a review see Pe'er & Ryde (2017), adopt the hydrodynamic model of a steady and infinite wind. However, finite duration of GRBs implies finite width of the wind. Winds of *finite duration* are classified as photon thin and photon thick (Bégué et al. 2013; Ruffini et al. 2013; Vereshchagin 2014). Decoupling of photons from plasma in the latter case occurs simultaneously in the entire outflow, while in the former case photons are transported to the boundaries of the outflow by radiative diffusion, just like in nonrelativistic outflows, e.g. in supernova ejecta. Emission in this case originates not at the photospheric radius, but at smaller radii. The photon thick case, corresponding to the steady wind, appears to be justified for typical GRB parameters. Photon thin regime is not considered in the literature, as it is assumed that at large radii the outflow is spreading (Piran et al. 1993; Mészáros et al. 1993) due

to strong velocity gradients initially present in the outflow, see e.g. (Piran et al. 1993; Mészáros et al. 1993). Such spreading outflows indeed correspond to the photon thick case (Ruffini et al. 2014). However, in absence of these gradients the outflow could be photon thin where decoupling of photons from expanding plasma occurs in the diffusive regime (Ruffini et al. 2013).

Radiative diffusion is known to be relevant for expanding ejecta in supernovae explosions (Arnett 1996), but was overlooked in the literature on GRBs. The purpose of the present work is to develop further the theory of photospheric emission (Ruffini et al. 2013), specifically focusing on the case when observed properties of such outflows are determined by the radiative diffusion of photons, and to confront it with the observational data.

The paper is organized as follows. The definition of the radius of photosphere is recalled in Section 2. Observational properties of diffusive photospheres are discussed in Section 3. The method allowing determination of initial radius and bulk Lorentz factor of the outflow is presented in Section 4. Observational properties of GRB cocoons are discussed in Section 5. Case studies of GRBs with thermal emission in the early afterglow is performed in Section 6. Discussion and conclusion follow. Appendix collects basic results for ultrarelativistic diffusive photospheres derived from the radiative transfer theory.

2 RELATIVISTIC PHOTOSPHERE

Consider a relativistic outflow launched at a radius R_0 . The outflow is characterized by its activity time Δt , the luminosity L and mass injection rate \dot{M} . The associated thickness of the outflow is $l = c\Delta t$. The entropy in the region where the energy is released is parametrized by a dimensionless parameter $\eta = L/Mc^2$. Spherical symmetry is assumed, but generalization for anisotropic case with $\eta(\theta)$, where θ is the polar angle is straightforward. When $\eta \gg 1$ the bulk Lorentz factor changes with the radial distance as

$$\Gamma \simeq \begin{cases} \frac{r}{R_0}, & R_0 < r < \eta R_0, \\ \eta \simeq \text{const}, & r > \eta R_0, \end{cases} \quad (1)$$

During both acceleration and coasting phases the continuity equation for the laboratory number density reduces to

$$n = \begin{cases} n_0 \left(\frac{R_0}{r}\right)^2, & R(t) < r < R(t) + l, \\ 0, & \text{otherwise,} \end{cases} \quad (2)$$

where $R(t)$ is the radial position of the inner boundary of the outflow.

The optical depth for a spherically symmetric outflow is (Abramowicz et al. 1991; Ruffini et al. 2013)

$$\tau = \int_R^{R+\Delta R} \sigma n (1 - \beta \cos \theta) \frac{dr}{\cos \theta}, \quad (3)$$

where $R + \Delta R$ is the radial coordinate at which the photon leaves the outflow, and θ is the angle between the velocity vector of the outflow and the direction of propagation of the photon, n is the laboratory number density of electrons and positrons, which may be present due to pair production. The dominant interaction of photons in our case is Compton scattering in the non-relativistic regime, so σ is the Thomson cross section.

Electron-positron-photon plasma with baryon loading reaches thermal equilibrium before its expansion starts (Aksenov et al.

2009, 2008). With decreasing entropy η opacity due to electrons associated with baryons increases and eventually dominates over pair opacity. For the laboratory density profile (2) one has in the radial direction

$$\tau = \begin{cases} \frac{1}{6} \tau_0 \left(\frac{R_0}{R}\right)^3, & R_0 \ll R \ll \eta R_0, \\ \frac{1}{2\eta^2} \tau_0 \left(\frac{R_0}{R}\right), & \eta R_0 \ll R \ll \eta^2 R_0, \\ \tau_0 \left(\frac{R_0}{R}\right)^2, & R \gg \eta^2 R_0, \end{cases} \quad (4)$$

where

$$\tau_0 = \frac{\sigma L}{4\pi m_p c^3 R_0 \eta} = n_0 \sigma R_0. \quad (5)$$

The first two lines correspond to a *photon thick outflow* and the third line corresponds to a *photon thin outflow* (Ruffini et al. 2013).

The photospheric radius R_{ph} is defined by equating (4) to unity

$$R_{ph} = \begin{cases} R_0 \left(\frac{\tau_0}{6}\right)^{1/3}, & \tau_0 \ll \eta^3, \\ R_0 \frac{\tau_0}{2\eta^2}, & \eta^3 \ll \tau_0 \ll 4\eta^4 \frac{l}{R_0}, \\ (\tau_0 R_0 l)^{1/2}, & \tau_0 \gg 4\eta^4 \frac{l}{R_0}. \end{cases} \quad (6)$$

In eqs. (4) and (6) the regions of validity of different approximations are expressed either for radius or for parameters of the outflow. The crucial parameter which determines whether the outflow is photon thick or thin is the ratio

$$\chi = \frac{\tau_0 l}{4\eta^4 R_0}. \quad (7)$$

The outflow is photon thin for $\chi \gg 1$ and it is photon thick otherwise.

3 RELATIVISTIC DIFFUSIVE PHOTOSPHERE

The definition of the photosphere implies that at this position in space the outflow as a whole becomes transparent to radiation. However, emission emerges from the outflow when it is optically thick as well. Such emission is due to radiative diffusion, which transfers the energy from deeper parts of the outflow towards its surface. Naively one can think that such an effect is negligible in ultrarelativistic outflows. However, this is not the case (Vereshchagin 2014). Indeed, the comoving time, which photon takes to cross the outflow with comoving thickness $l_c = \Gamma l$ is $t_c = l_c^2/D_c$, where $D_c = c/3\sigma n_c$ is the diffusion coefficient, $n_c = n/\Gamma$ is the comoving density of the outflow. The radial coordinate of the outflow at this time is $R \simeq \Gamma c t_c$.

This diffusion radius is found in (Ruffini et al. 2013), and it is given by

$$R_D = \left(\tau_0 \eta^2 R_0 l^2\right)^{1/3}, \quad (8)$$

where eq. (5) has been used. It turns out to be always smaller than the photospheric radius of photon thin outflow, $R_D \ll R_{ph}$, so the radiation escapes such an outflow before it becomes transparent, just like in the supernova ejecta. In this sense the characteristic radius of the photospheric emission is not the photospheric radius

found from (4), but the radius of diffusion (8). The probability distribution of last scattering of photons in diffusive photospheres is qualitatively different from the usual photospheric emission (Bégué et al. 2013). Besides, the comoving temperature of escaping radiation is different from the temperature at the photospheric radius. Applicability of the photon thin asymptotics, last line in eq. (6), can be written using eq. (8) as

$$l \ll \frac{R_D}{\sqrt{2}\eta^2}. \quad (9)$$

For larger thickness l photon thin asymptotics disappears, so in the limit $l \rightarrow \infty$ the stationary wind with photon thick asymptotics is recovered.

Adiabatic expansion implies (Ruffini & Vereshchagin 2013) that the observed temperature of the outflow does not change while it is accelerating, and it decreases as $T_{obs} \propto R^{-2/3}$ at the coasting phase. Taking into account finite size of emitter and cosmological redshift one has (Pe'er et al. 2007)

$$T_{obs} = \frac{\xi}{1+z} T_0 \left(\frac{\eta R_0}{R_D} \right)^{2/3}, \quad (10)$$

where ξ is a numerical factor of order unity, z is cosmological redshift. In estimates below $\xi = 1.48$ is assumed following (Pe'er et al. 2007), which is found from the Monte Carlo simulations in the infinite wind approximation, though the value of ξ in the acceleration phase and in the photon thin case could be slightly different. The temperature at the base of the outflow is

$$T_0 \simeq \left(\frac{L}{4\pi c a R_0^2} \right)^{1/4}, \quad (11)$$

where $a = 4\sigma_{SB}/c$ is the radiation constant, σ_{SB} is the Stefan-Boltzmann constant. Finally, the duration of photospheric emission for a distant observer is

$$t_a^D = (1+z) \frac{R_D}{2\eta^2 c}. \quad (12)$$

In the photon thick case the duration of thermal emission is determined by the width of the outflow l , which is unconstrained. In the photon thin case this duration is given by eq. (12) and it is a function of the diffusion radius and the Lorentz factor.

The luminosity of photospheric component scales with radius as

$$L_{ph} = L_0 \left(\frac{\eta R_0}{R} \right)^{8/3}, \quad (13)$$

and the applicability condition of the photon thin case in eq. (6) and together with the definition of diffusion radius in eq. (8) imply for the luminosity of diffusive photosphere

$$L_{thin} < L_0 \left(\frac{R_0}{\eta l} \right)^{8/3} \ll L_0. \quad (14)$$

This means that thermal emission is much weaker than the emission of the prompt radiation, if γ -rays are produced with high efficiency there. For $l \sim R_0$ this condition strongly favours small values of η and, consequently, small Lorentz factors of the outflow.

4 DETERMINATION OF INITIAL RADIUS AND BULK LORENTZ FACTOR OF THE OUTFLOW

Assuming that the observed thermal component in early afterglows of some GRBs is of photospheric origin, one can estimate initial

radius of the outflow directly from observations (Pe'er et al. 2007). Indeed, in the ultrarelativistic regime one has

$$\mathcal{R} \equiv \left(\frac{F_{obs}^{BB}}{\sigma_{SB} T_{obs}^4} \right)^{1/2} = \zeta \frac{(1+z)^2 R}{d_L \Gamma}, \quad (15)$$

where R is the emission radius, d_L is the luminosity distance, ζ is a numerical factor of order unity. Following (Pe'er et al. 2007) $\zeta = 1.06$ is assumed for the estimates below. In Pe'er et al. (2007) the emission radius R was associated with the photosphere of the *photon thick* outflows. However, this relation is valid for any ultrarelativistic emitter. Therefore, from eqs. (10), (15) and (11) the initial radius is

$$R_0 = \frac{4^{3/2} d_L}{\xi^6 \zeta^4 (1+z)^2} \mathcal{R} \left(\frac{F_{obs}^{BB}}{Y F_{obs}} \right)^{3/2}. \quad (16)$$

In the derivation of this results only two assumptions are made. First, the outflow should be coasting at ultrarelativistic speed, $\Gamma = \eta \gg 1$. Secondly, the relation $L = 4\pi d_L^2 Y F_{obs}$ is used, where Y is the fraction of the total luminosity L and the energy emitted in X and γ -rays in the prompt phase.

In addition to the initial radius R_0 an equation for the Lorentz factor can be obtained. Since the emitter radius for the *photon thin* outflows is the diffusion radius $R = R_D$, from eqs. (8) and (15) one obtains, see also (Bégué & Iyyani 2014)

$$\frac{\eta}{l} = \frac{\zeta^{3/2} (1+z)^3}{d_L^{1/2}} \left(\frac{\sigma Y F_{obs}}{m_p c^3 \mathcal{R}^3} \right)^{1/2}. \quad (17)$$

Therefore, the Lorentz factor can be determined if l is known. In particular case $l = R_0$ from (17) it follows the minimum Lorentz factor for which the photon thin case applies

$$\eta_{thin} = (1+z) \left(d_L \frac{Y F_{obs} \sigma}{m_p c^3 \mathcal{R}} \right)^{1/2} \frac{4^{3/2}}{\zeta^{5/2} \xi^6} \left(\frac{F_{obs}^{BB}}{Y F_{obs}} \right)^{3/2}. \quad (18)$$

The condition (9) determines the applicability limit of the photon thin case, so for $\sqrt{2}\eta^2 l = R_D$ the photon thick case is recovered (Pe'er et al. 2007)

$$\eta_{thick} = \left[\zeta (1+z)^2 d_L \frac{\sigma Y F_{obs}}{m_p c^3 \mathcal{R}} \right]^{1/4}. \quad (19)$$

Equations (17) and (18) allow the determination of the bulk Lorentz factor of the *photon thin* outflow, provided the measurement of the total flux F_{obs} and the parameter \mathcal{R} . Comparing eqs. (18) and (19) leads to the conclusion that the Lorentz factor inferred from the photon thin asymptotics is typically smaller than the one of the photon thick case; besides, it contains the inverse of the Y parameter, unlike a factor $Y^{1/4}$ in the latter case.

It is important to stress that from the theoretical point of view, given the total luminosity and the initial radius of the outflow one cannot distinguish between photon thick and photon thin cases as both sets of parameters are possible with different η and photospheric radius. These parameters are related by eq. (15), therefore independent observational information is required in order to differentiate between the two cases.

5 GRB COCOONS

Consider typical parameters relevant for GRB jets which is penetrating the progenitor (Nakar & Piran 2017). In what follows introduce the notation $A_x = A/10^x$, so the luminosity L_{52} stands for 10^{52} erg/s, which is the isotropic luminosity. While the entropy of the jet can take large values, the mixing between the progenitor and the jet

lowers the entropy of the cocoon, so $\eta = 10$ is chosen, as a reference value. It is also likely that the entropy is a decreasing function of the angular distance from the jet. Assume that initial radius of the wind R_0 is given by the radius of the core of the progenitor WR star $R_0 \sim 10^9$ cm, and the thickness of the wind corresponds to the size of the WR star $l_{12} = 10^{12}$ cm (Crowther 2007). The crucial parameter which determines whether the outflow is photon thick or thin is the ratio

$$\chi \simeq 29L_{52}l_{12}^{-1}\eta_1^{-5}. \quad (20)$$

For $\chi \gg 1$ the outflow is photon thin, which is the case for our fiducial parameters. Considering the extreme dependence on η , for smaller η the condition is clearly satisfied. Hence the cocoon is in the photon thin regime and therefore the radiation from the cocoons is governed by radiative diffusion. The diffusion radius is

$$R_D \simeq 4.9 \times 10^{14} L_{52}^{1/3} \eta_1^{1/3} l_{12}^{2/3} \text{ cm}, \quad (21)$$

and the arrival time corresponding to this radius is

$$t_a^D = (1+z) \frac{R_D}{2\eta^2 c} \simeq 81.7(1+z)L_{52}^{1/3} \eta_1^{-5/3} l_{12}^{2/3} \text{ s}, \quad (22)$$

which is the typical duration of thermal emission observed in early afterglows of GRBs.

The observed temperature at the diffusion radius is

$$T_{obs} = 0.12L_{52}^{1/36} R_9^{1/6} \eta_1^{4/9} l_{12}^{-4/9} \text{ keV}, \quad (23)$$

which is also a typical temperature of thermal emission in early afterglows of GRBs (Valan et al. 2018).

Such inferred values of temperature and duration call for closer attention to the radiation properties of photon thin outflows.

6 CASE STUDIES

All GRBs reported in Valan et al. (2018) with measured redshifts and thermal component detected in their early afterglows were considered, namely GRBs 060218, 090618, 101219B, 111123A, 111225A, 121211A, 131030A, 150727A, 151027A. Observed temperature, thermal flux and total flux were averaged for the entire duration of the thermal emission. The initial radius was found from eq. (16). Two values of the Lorentz factor in photon thin, eq. (18), and photon thick, eq. (19), cases were determined. Then the minimum value of the Y parameter is found which allows the duration of the photospheric emission (12) to be not less than the observed duration of the thermal component. The values are reported in Tab. A1. Only six cases allow both photon thick and photon thin interpretations for the photosphere; for other cases photon thin case does not apply because eq. (19) gives smaller Lorentz factor than eq. (18).

GRB 060218. This is a well studied nearby GRB (Campana et al. 2006) with record breaking duration of the thermal signal interpreted as the break out of a shock driven by a mildly relativistic shell into the dense wind surrounding the progenitor, see however (Ghisellini et al. 2007; Emery et al. 2019). The thermal emission in this burst with observed temperature $T_{BB} = 0.15$ keV may be also explained as a photosphere of a cocoon launched from initial radius 3.18×10^{11} cm with a mildly relativistic Lorentz factor $1.2Y^{-1} < \Gamma < 1.6Y^{1/4}$ emitting in the photon thin regime. This estimate of the Lorentz factor is in agreement with radio observation at 2 days, requiring $\Gamma \sim 2$ (Soderberg et al. 2006). Given that the condition $\Gamma \gg 1$ is not satisfied, results of the theory of diffusive ultrarelativistic photospheres can be applied to this case with great

care. In particular, the estimated duration of the thermal signal is only 13Y s.

GRB 090618. This burst may represent a canonical case of photon thin outflow launched from the initial radius 10^9 cm with the Lorentz factor $3Y^{-1} < \Gamma < 40Y^{1/4}$. Assuming instantaneous energy injection with $l = R_0$ one finds $Y = 5.7$. The duration of the thermal emission with observed temperature about 1 keV is about 6Y s. Note that thermal emission has also been claimed in the prompt phase, with a higher temperature ranging from 54 to 12 keV (Izzo et al. 2012). Such thermal emission in the prompt phase may be interpreted as a photosphere of the photon thick outflow. Indeed, if the initially high entropy η decreases with time the outflow should experience a transition from photon thick to photon thin case.

GRB 111225A. This case is similar to GRB 060218, but with smaller initial radius of 8.3×10^9 cm and Lorentz factor in the range $1 < \Gamma < 6.0Y^{1/4}$. The duration of the thermal emission with observed temperature of 0.18 keV is about 126Y s, with $Y = 2.0$ for $l = R_0$. The lower bound on the Lorentz factor is unconstrained. It may correspond to a cocoon emitting in the diffusive photon thin regime.

GRB 131030A. This case is a typical long burst, similar to GRB 090618, it allows Lorentz factors in the photon thin case in the following range: $4.3Y^{-1} < \Gamma < 66Y^{1/4}$. The duration of the thermal emission with observed temperature of 1.12 keV is about 2.0Y s. The initial radius is 3.74×10^8 cm. For instantaneous energy injection $Y = 19$.

GRB 150727A. This case is similar to GRB 111225A with initial radius 1.1×10^9 cm and Lorentz factors in the range $1 < \Gamma < 11Y^{1/4}$, allowing for a photon thin interpretation. The duration of the thermal emission with observed temperature of 0.47 keV is about 191Y s, with $Y = 2.1$.

GRB 151027A. This case is similar to GRBs 090618 and 131030, however with quite large initial radius 1.5×10^{10} cm and Lorentz factors in the narrow range $23 < \Gamma < 26Y^{1/4}$. The duration of the thermal emission with observed temperature of 0.96 keV is about 0.47Y s, with $Y = 64$.

7 DISCUSSION

The difference between the present work and the approach followed by Pe'er et al. (2006) should be emphasized. The main assumption of that work is the presence of unknown dissipation mechanism, which transforms part of the kinetic energy of the outflow into radiation, postulated in (Rees & Mészáros 2005). Such dissipation can boost the luminosity of thermal emission and it might be required to explain subdominant thermal component during the prompt emission or even the prompt emission itself, see (Bhattacharya & Kumar 2020). Concerning observations of this component in the early afterglow, dissipation is not required, as it is much weaker than the prompt radiation.

Similarly, there is a difference between the present work and the work by Nakar & Piran (2017). There two regimes of expansion are considered: Newtonian ($v < c$) and ultrarelativistic $\eta \gg 1$. For the latter, which is of interest here, the emission was assumed to originate at the photospheric radius, given by the last line in eq. (6). As discussed in Sec. 3 above, photons in this case diffuse out much earlier, so that no photons are left in the outflow when it arrives to the photospheric radius. For this reason estimations of the luminosity and observed temperature in that paper cannot be used.

Qualitative difference in dependence of observed flux and temperature on time for photon thin outflows determine their ob-

served properties. In particular, since the flux up to diffusion time (22) is almost constant, see eq. (B11) in Appendix, and its luminosity is much weaker than the prompt radiation luminosity, see eq. (14), the thermal component become visible after the steep decrease of observed luminosity following the end of the prompt phase. This is indeed where such thermal component is identified in many GRBs. Its disappearance is naturally explained by diffusion of the radiation kept in the outflow. Hence it implies that no more photons are generated neither in the outflow nor in the central engine.

The results of the present work indicate that in several GRBs, namely GRB 060218, 111225A and 150727A, the thermal component observed in the early afterglow may originate from mildly relativistic cocoons emerging from the progenitors together with the jet, due to relatively small values of inferred Lorentz factors $\Gamma < 10$. At the same time, such emission observed in GRBs 090618, 131030A and 151027A correspond to large Lorentz factors $\Gamma > 10$, indicating a jet origin of the photospheric emission. Besides, these results suggest that the progenitors of some long GRBs, in particular GRB 090618 and 131030A could be rather compact objects, with radius $l \sim 10^9$ cm.

It is important to stress that the relatively low temperature of the thermal component observed in the early afterglow with $T \sim 0.1 - 10$ keV, in contrast with typical temperatures detected during the prompt emission with $T \sim 10 - 100$ keV does not indicate small Lorentz factor of the outflow. Conversely, it may point to photospheric origin of the thermal emission in the photon thin regime. Instead, large Lorentz factors $\Gamma \gg 1$ assumed in the model imply small mass of the emitting plasma, which is consistent with the cocoon interpretation (Nakar & Piran 2017).

Possible presence of thermal components both in the prompts radiation and in the early afterglow, as well as the presence of breaks in temperature dependence on time found in many cases (Ryde 2004, 2005; Ryde & Pe'er 2009) may correspond to the transition from photon thick to photon thin asymptotics in hydrodynamic evolution of the outflow powering GRBs.

8 CONCLUSIONS

The theory of diffusive emission from relativistic photospheres is developed and confronted with observational data on a sample of GRBs with thermal component in the early afterglows. The measurement of temperature and flux of the thermal component along with the total flux in the prompt phase are used to determine initial radii of the outflows as well as their Lorentz factors.

The results indicate that in several cases (GRBs 060218, 111225A and 150727A) the inferred Lorentz factors are relatively small, $\Gamma < 10$, while in other cases (GRBs 090618, 131030A and 151027A) the inferred Lorentz factors are larger, $\Gamma > 10$. Such differences suggest two possible sources of the thermal component: mildly relativistic cocoons or highly relativistic jets. This is valid only for those cases, where inferred Lorentz factor is relatively small, below few tens. For other cases identified in Valan et al. (2018) inferred Lorentz factors are larger, and photon thin interpretation does not apply.

These results are the first indication that radiative diffusion may play an important role not only in nonrelativistic outflows, but also in ultrarelativistic outflows, represented by GRBs.

Acknowledgements. It is a pleasure to thank Dr. Damien Bégué for careful reading of the manuscript and useful comments.

REFERENCES

- Abramowicz M. A., Novikov I. D., Paczynski B., 1991, *ApJ*, **369**, 175
 Aksenov A. G., Ruffini R., Vereshchagin G. V., 2008, in American Institute of Physics Conference Series. pp 191–196, doi:10.1063/1.2836994
 Aksenov A. G., Ruffini R., Vereshchagin G. V., 2009, *Phys. Rev. D*, **79**, 043008
 Arnett D., 1996, *Supernovae and Nucleosynthesis: An Investigation of the History of Matter from the Big Bang to the Present*. Princeton University Press
 Barthelmy S. D., et al., 2013, GRB Coordinates Network, **15456**, 1
 Baumgartner W. H., et al., 2011, GRB Coordinates Network, **12726**, 1
 Bégué D., Iyyani S., 2014, *ApJ*, **792**, 42
 Bégué D., Siutsou I. A., Vereshchagin G. V., 2013, *ApJ*, **767**, 139
 Beloborodov A. M., 2011, *ApJ*, **737**, 68
 Bhattacharya M., Kumar P., 2020, *MNRAS*, **491**, 4656
 Bhattacharya M., Lu W., Kumar P., Santana R., 2018, *ApJ*, **852**, 24
 Campana S., et al., 2006, *Nature*, **442**, 1008
 Cenko S. B., Perley D. A., Jankkarinen V., Burbidge M., Diego U. S., Miller K., 2009, GRB Coordinates Network, **9518**, 1
 Crowther P. A., 2007, *ARA&A*, **45**, 177
 Emery S. W. K., Page M. J., Breeveld A. A., Brown P. J., Kuin N. P. M., Oates S. R., De Pasquale M., 2019, *MNRAS*, **484**, 5484
 Foley R. J., Bloom J. S., Perley D. A., Butler N. R., 2006, GRB Coordinates Network, **5376**, 1
 Friis M., Watson D., 2013, *The Astrophysical Journal*, **771**, 15
 Ghisellini G., Ghirlanda G., Tavecchio F., 2007, *Monthly Notices of the Royal Astronomical Society: Letters*, **382**, L77
 Haskell R. C., Svaasand L. O., Tsay T.-T., Feng T.-C., McAdams M. S., Tromberg B. J., 1994, *Journal of the Optical Society of America A*, **11**, 2727
 Izzo L., et al., 2012, *A&A*, **543**, A10
 Izzo L., et al., 2019, *Nature*, **565**, 324
 Lundman C., Pe'er A., Ryde F., 2013, *MNRAS*, **428**, 2430
 Mészáros P., Rees M. J., 2000, *ApJ*, **530**, 292
 Mészáros P., Laguna P., Rees M. J., 1993, *ApJ*, **415**, 181
 Nakar E., Piran T., 2017, *ApJ*, **834**, 28
 Page K. L., et al., 2011, *Monthly Notices of the Royal Astronomical Society*, **416**, 2078
 Palmer D. M., et al., 2015, GRB Coordinates Network, **18496**, 1
 Pe'er A., 2008, *ApJ*, **682**, 463
 Pe'er A., Ryde F., 2011, *ApJ*, **732**, 49
 Pe'er A., Ryde F., 2017, *International Journal of Modern Physics D*, **26**, 1730018
 Pe'er A., Meszaros P., Rees M. J., 2006, *The Astrophysical Journal*, **652**, 482
 Pe'er A., Ryde F., Wijers R. A. M. J., Mészáros P., Rees M. J., 2007, *ApJ*, **664**, L1
 Perley D. A., Hillenbrand L., Prochaska J. X., 2015, GRB Coordinates Network, **18487**, 1
 Piran T., Shemi A., Narayan R., 1993, *MNRAS*, **263**, 861
 Rees M. J., Meszaros P., 1994, *ApJ*, **430**, L93
 Rees M. J., Mészáros P., 2005, *ApJ*, **628**, 847
 Ruffini R., Vereshchagin G., 2013, *Il Nuovo Cimento*, **C 36**, 255
 Ruffini R., Siutsou I. A., Vereshchagin G. V., 2013, *The Astrophysical Journal*, **772**, 11
 Ruffini R., Siutsou I. A., Vereshchagin G. V., 2014, *New Astronomy*, **27**, 30
 Ruffini R., Vereshchagin G. V., Wang Y., 2017, *A&A*, **600**, A131
 Rybicki G. B., Lightman A. P., 1979, *Radiative processes in astrophysics*. Springer
 Ryde F., 2004, *ApJ*, **614**, 827
 Ryde F., 2005, *ApJ*, **625**, L95
 Ryde F., Pe'er A., 2009, *ApJ*, **702**, 1211
 Ryde F., et al., 2010, *ApJ*, **709**, L172

6 *Vereshchagin and Siutsou*

- Ryde F., Lundman C., Acuner Z., 2017, *MNRAS* , 472, 1897
- Sakamoto T., et al., 2006, GRB Coordinates Network, 4822, 1
- Sakamoto T., Ukwatta T. N., Barthelmy S. D., 2009, GRB Coordinates Network, 9534, 1
- Santana R., Crumley P., Hernández R. A., Kumar P., 2016, *MNRAS* , 456, 1049
- Soderberg A. M., et al., 2006, *Nature* , 442, 1014
- Sparre M., Starling R. L. C., 2012, Monthly Notices of the Royal Astronomical Society, 427, 2965
- Stamatikos M., et al., 2015, GRB Coordinates Network, 18086, 1
- Starling R. L. C., Page K. L., Pe'er A., Beardmore A. P., Osborne J. P., 2012, Monthly Notices of the Royal Astronomical Society, 427, 2950
- Tanvir N. R., Xu D., Zafar T., Covino S., Schulze S., 2015, GRB Coordinates Network, 18080, 1
- Thoene C. C., de Ugarte Postigo A., 2014, GRB Coordinates Network, 16079, 1
- Valan V., Larsson J., Ahlgren B., 2018, *MNRAS* , 474, 2401
- Vereshchagin G. V., 2014, *International Journal of Modern Physics D*, 23, 1430003
- Xu D., Fynbo J. P. U., Jakobsson P., Cano Z., Milvang-Jensen B., Malesani D., de Ugarte Postigo A., Hayes M., 2013, GRB Coordinates Network, 15407, 1
- Zhang B., 2018, *The Physics of Gamma-Ray Bursts*. Cambridge University Press, doi:10.1017/9781139226530

Table A1. Results of calculation of Lorentz factors and initial radii for the set of GRBs from Valan et al. (2018). Reported are: GRB name, redshift, fluence, duration of the prompt emission T_{90} , duration of the thermal component Δt_{BB} , estimated duration of the photospheric emission Δt , average observed temperature T_{BB} , Lorentz factor of the photon thick case, Lorentz factor of the photon thin case, initial radius R_0 and the references: [1] (Sakamoto et al. 2006; Foley et al. 2006); [2] (Sakamoto et al. 2009; Cenko et al. 2009); [3] (Baumgartner et al. 2011; Thoene 2014); [4] (Barthelmy et al. 2013; Xu et al. 2013); [5] (Tanvir et al. 2015; Stamatikos et al. 2015); [6] (Palmer et al. 2015; Perley et al. 2015).

GRB	z	Fluence, erg/cm ²	T_{90} , s	Δt_{BB} , s	Δt , s	T_{BB} , keV	η_{thick}	η_{thin}	R_0 , 10 ¹⁰ cm	Y	Reference
060218	0.033	6.8×10^{-6}	> 2000	2624	13 Y	0.146	$1.6Y^{1/4}$	$1.2Y^{-1}$	$32Y^{-3/2}$	206	[1]
090618	0.54	2.7×10^{-4}	113.2	34	6.0 Y	1.05	$40Y^{1/4}$	$3.0Y^{-1}$	$0.094Y^{-3/2}$	5.7	[2]
111225A	0.297	1.3×10^{-6}	106.8	331	126 Y	0.18	$6.0Y^{1/4}$	> 1	$0.83Y^{-3/2}$	2.0	[3]
131030	1.293	6.6×10^{-5}	41	90	2.0 Y	1.12	$66Y^{1/4}$	$4.3Y^{-1}$	$0.037Y^{-3/2}$	19	[4]
150727A	0.313	7.9×10^{-6}	88	518	191 Y	0.25	$11Y^{1/4}$	> 1	$0.11Y^{-3/2}$	2.1	[5]
151027A	0.81	1.94×10^{-5}	130	55	0.47 Y	0.96	$26Y^{1/4}$	$23Y^{-1}$	$1.5Y^{-3/2}$	64	[6]

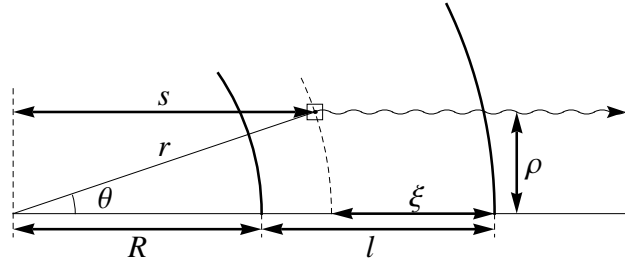


Figure B1. Geometry of the outflow and variables used. Observer is located to the right at infinity.

APPENDIX A: INITIAL RADIUS AND LORENTZ FACTORS IN PHOTON THICK AND PHOTON THIN CASES

In Tab. A1 results of calculations of the initial radius R_0 and Lorentz factors η in photon thick and photon thin cases. The sample of GRBs with thermal component detected in the early afterglows of GRBs is adopted from (Valan et al. 2018). Both flux and observed temperature reported in online material of that paper for time resolved intervals are averaged on the entire duration of observation of thermal component.

APPENDIX B: EMISSION FROM PHOTON THIN OUTFLOWS

Recall the solution of the radiative transfer equation for photon thin outflows in diffusion approximation (Ruffini et al. 2013). The radiative transfer equation for specific intensity I_ν along the ray (see e.g. (Rybicki & Lightman 1979), p. 11) is

$$\frac{dI_\nu}{ds} = j_\nu - \kappa_\nu I_\nu, \quad (\text{B1})$$

where j_ν is monochromatic emission coefficient for frequency ν , κ_ν is absorption coefficient and s is distance, measured along the ray, see Fig. B1.

Spectral intensity of radiation at infinity on a ray coming to observer at some arrival time t_a is given by formal solution of this equation (Beloborodov 2011)

$$I_\nu(\nu, \rho, t_a) = \int \mathcal{I}_\nu(\nu, r, \theta, t) \exp[-\tau(\nu, r, \theta, t)] d\tau, \quad (\text{B2})$$

where $\mathcal{I}_\nu(r, \theta, t) = j_\nu/\kappa_\nu$ is the source function and the optical depth is

$$\tau = \int_s^\infty \kappa_\nu ds, \quad (\text{B3})$$

and variables (r, θ, t) are connected by $t_a = t - (r/c) \cos \theta$ and $\rho = r \sin \theta$, see Fig. B1.

The total observed flux is

$$F_\nu(\nu, t_a) = 2\pi \Delta\Omega \int I_\nu(\nu, \rho, t_a) \rho d\rho, \quad (\text{B4})$$

where $\Delta\Omega$ is the solid angle of the observer's detector as seen from the outflow in the laboratory frame and $2\pi \rho d\rho$ is an element of area in the plane of the sky.

That emissivity j_ν is assumed to be thermal and isotropic in comoving frame and $\kappa_{\nu,c} = \text{const}$. The laboratory source function is then

$$\mathcal{I}_\nu(\nu, r, \theta, t) = \frac{2h}{c^2} \frac{\nu^3}{\exp\left(\frac{h\nu\Gamma(1-\beta\cos\theta)}{kT_c(r,t)}\right) - 1}, \quad (\text{B5})$$

where h is the Planck constant. The source function \mathcal{I} depends on both r and t . The Rosseland radiative diffusion approximation is used (see e.g. (Rybicki & Lightman 1979), pp. 39–42). It is useful to introduce the function $L_c(\xi, t) = (t/t_0)^{8/3} I_c(\xi, t)$, which accounts for the adiabatic cooling of radiation in expanding outflow. Here both ξ and time t are measured in the laboratory frame, while $I_c(\xi, t)$ is measured in the comoving frame. By applying multipolar decomposition the diffusion equation was derived from (B1) in the ultrarelativistic limit (Ruffini et al. 2013)

$$\frac{\partial L}{\partial ct} - \frac{c^2 t^2 \Delta}{3R_0} \frac{\partial^2 L}{\partial \xi^2} = 0, \quad \Delta = \frac{1}{\Gamma^2 \tau_0}. \quad (\text{B6})$$

Notice that the diffusion coefficient is explicitly time dependent due to the expansion of the outflow.

This equation should be supplemented with boundary conditions. There are two types of boundary conditions used frequently: free-streaming, for example in two-stream approximation ((Rybicki & Lightman 1979), pp. 42–45), and zero boundary conditions, that can be used as replacement for free-streaming for “extrapolated boundary” (Haskell et al. 1994). The position of “extrapolated boundary” is found as $\xi = -k \frac{c^2 t^2 \Delta}{R_0}$ (k is a constant of order unity, dependent on the approximation used for free-streaming description), and for the main part of emission it is very close to the real boundary. In the case of zero boundary conditions $L|_{\xi=0} = L|_{\xi=l} = 0$ there is a series expansion of solution, that for initial conditions $L(\xi, t_0) = 1$ gives

$$L_c(\xi, t) = \sum_{n=0}^{\infty} \frac{4}{(2n+1)\pi} \exp\left[-\frac{\Delta(2n+1)^2 \pi^2 c^3 (t^3 - t_0^3)}{9R_0^3}\right] \times \sin\left[\frac{(2n+1)\pi\xi}{l}\right]. \quad (\text{B7})$$

This solution in comparison with numerical one with free-streaming boundary conditions is accurate to a few percent. The corresponding flux is characterized by an initial burst and then tends to the asymptotic solution, that corresponds to $t_0 = 0$. with the flux

$$F_c(t) = \frac{4t^2}{3t_D^2} \vartheta_2\left[0, \exp\left(-\frac{4\pi^2}{9} \left(\frac{t}{t_D}\right)^3\right)\right], \quad (\text{B8})$$

where ϑ_2 is the Jacobi elliptic theta function. The raising part of the corresponding flux of L_c through the external boundary of the outflow scales as $t^{1/2}$, while its decaying part is quasi-exponential one. The peak of the flux is near the diffusion time

$$t_D = \frac{R_0}{c} \Delta^{-1/3}, \quad (\text{B9})$$

and “extrapolated boundary” $\xi = -kR_0\Delta^{-1/3} \ll R_0$ is very close to real one as $\Delta \ll 1$, that ensures the accuracy of (B7). For practical purpose it is possible to write a simpler expression

$$F_c(t) = \frac{9}{8} \left(\frac{t}{t_D}\right)^{1/2} \exp\left[-\frac{4}{9} \left(\frac{t}{t_D}\right)^4\right], \quad (\text{B10})$$

which accurately describe both raising and decaying parts of the flux. The observed flux as function of arrival time is obtained from (B8) by integrating over the emitting surface, which gives a factor $(t/t_0)^2$, and by correcting for adiabatic factor, which gives additional factor $(t/t_0)^{-8/3}$, so the final expression is

$$F_{obs}(t_a) = \frac{9}{8} \left(\frac{t}{t_a^D}\right)^{-1/6} \exp\left[-\frac{4}{9} \left(\frac{t}{t_a^D}\right)^4\right]. \quad (\text{B11})$$

This result is in sharp contrast with strongly decreasing flux from photon thick outflows $F_{obs}(t_a) \propto t_a^{-2}$ (Pe’er & Ryde 2011; Ruffini et al. 2013).

The comoving temperature of radiation on the photosphere is determined by the balance between the energy diffusion from the interior of the outflow and radiative losses and it is much smaller than the temperature in the interior. The variation of observed temperature across the emitting surface is small and hence the observed instantaneous spectrum is very close to the thermal one and peaks near the observed temperature on the line of sight. Observed temperature is determined from the observed flux (B11) as $F \propto R^2 T^4$ and the result is

$$T_{obs}(t_a) = T_D \left(\frac{t}{t_D}\right)^{-13/24} \exp\left[-\frac{t}{t_a^D}\right], \quad (\text{B12})$$

which reflects the fact that for $t > t_D$ the observed temperature decreases exponentially. This result is in contrast with a power law decrease of observed temperature of photon thick outflows $T_{obs}(t_a) \propto t_a^{-2/3}$ (Pe’er & Ryde 2011; Ruffini et al. 2013).